Quantitative determination of the monoclinic crystalline phase content in polyethylene by ^{13}C n.m.r.

D. L. VanderHart and F. Khoury
National Bureau of Standards, Washington, DC 20234, USA
(Received 14 February 1984)

Solid-state ^{13}C n.m.r. spectroscopy involving the techniques of cross-polarization (CP), magic angle spinning (MAS), and high power proton decoupling, has been used to determine quantitatively the ratio of monoclinic to orthorhombic crystalline phases in compression moalded ultra-high molecular weight polyethylene (UHMWPE) sheet which had been stretched uniaxially. Criteria for expecting quantitative relative intensities in ^{13}C CP-MAS spectra are discussed. Attenuation of the non-crystalline (NC) signals relative to crystalline signals was observed. Experiments were therefore carried out to ascertain whether measurable relative intensity distortions exist between the monoclinic crystalline phase (MCP) and the orthorhombic crystalline phase (OCP) resonances due to possible differences in proton 'spin diffusion' between the NC and the two crystalline phases during cross-polarization. No relative intensity distortions were detected. This result, coupled with experiments in which spin diffusion was monitored at times longer than those used for cross-polarization, suggests that the average distance from the protons in a given crystalline phase to the nearest protons in the NC regions is the same for the MCP and the OCP. Finally, non-spinning ^{13}C spectra of the deformed polyethylene were recorded to determine the orientation of the chains in the crystalline and NC regions. The Hermans orientation function, F_c, was determined independently for the crystalline (combined OCP and MCP) and NC regions, and found to be $0.66+0.06$ and $0.23+0.04$ respectively. The occurrence of orientation in the NC regions may be evidence for internal stresses, which, it is suggested, also stabilize the metastable MCP in the stretched sample.

(Keywords: to follow)

INTRODUCTION

Polyethylene deformed under certain conditions contains regions of a metastable crystalline phase[1-15] in addition to the familiar orthorhombic crystalline[16] phase (OCP) and the non-crystalline) disordered) regions (NC). The metastable phase is crystalographically distinct from the OCP and its presence in strained specimens is revealed by the occurrence of characteristic 'extra' reflections in wide angle X-ray[1-10] and electron diffraction patterns[11-13]. It has also been detected by i.r. spectroscopy[14]. This phase has, of late, been referred to as the monoclinic crystalline phase (MCP) after the unit cell proposed by Seto *et al.*[8] which followed earlier proposals, based on more limited X-ray diffraction data, that the structure was triclinic[5,7].

The environments of the methylene groups in the MCP and the OCP are distinctly different from one another. The main feature which distinguishes the monoclinic structure proposed by Seto *et al.*[8] (as well as the earlier triclinic cells[5,7]) from the orthorhombic unit cell of polyethylene[16] is that the planes of the zig-zag (all-*trans*) chains in the MCP are parallel to one another, as is the case of the n-alkanes n-C_yH_{2y+2} with $6 \leqslant y(\text{even}) < 26$ whose unit cells are triclinic and contain one chain per cell[17-20]. In contrast, the angle between the planes of the two all-*trans* chains which traverse the orthorhombic cell of polyethylene is close to 90°[16], as is the case in the orthorhombic subcell of both the monoclinic and/or orthorhombic n-alkanes with $26 \leqslant y(\text{even}) \leqslant 100$[19-24] and in the orthorhombic n-alkanes with $11 \leqslant y(\text{odd}) \leqslant 39$[19,20,25].

Our main objective in this paper is to introduce solid state ^{13}C n.m.r. as a method for detecting the presence of the MCP in polyethylene, as well as a quantitative tool for assessing the ratio of MCP to OCP in bulk specimens of polyethylene. An advantage of the method is that it is independent of the orientations of the phases in the specimens.

The possibility that ^{13}C n.m.r. could serve as a diagnostic tool for distinguishing between the MCP and the OCP in polyethylene followed naturally from results of a previous study of representative n-alkanes with different crystal structures using magic angle spinning (MAS) ^{13}C n.m.r.[26]. In that study[26] n-$C_{19}H_{40}$, n-$C_{20}H_{42}$, n-$C_{23}H_{48}$ and n-$C_{32}H_{66}$ (referred to as C-19, C-20, C-23 and C-32) were chosen as examples typifying the pseudo-hexagonal (high temperature), triclinic, orthorhombic and monoclinic forms of the n-alkanes respectively. It was found that the isotropic chemical shifts of the interior methylene carbons in these n-alkanes were the same, except in the case of the triclinic C-20 in which a downfield deviation of 1.3 ± 0.4 p.p.m. in the methylene resonance was observed. Although the precise origin of this shift is not well understood, its manifestation can be reasonably taken as a signature diagnostic of the n-alkanes in which the planes of the zig-zag chains are parallel to one another as is the case in triclinic C-20. Accordingly, since, as indicated

0032-3861/84/111589-11$03.00

above, this latter feature is also a characteristic of the MCP in polyethylene which distinguishes it from the OCP, it seemed reasonable to expect that in the case of polyethylene the methylene ^{13}C resonance of the MCP would be shifted downfield relative to that of the OCP by approximately 1.3 ppm.

The stimulus for testing this conjecture stemmed from an investigation of aspects of the morphology and mechanical properties of compression moulded sheets of UHMWPE[27-29]. Wide angle X-ray diffraction (WAXD) patterns taken during the course of that study revealed the presence of the MCP in addition to the OCP in sheets which had been stretched uniaxially[27-29]. There was, however, no detectable evidence of the MCP in the unstrained sheets. The availability of the samples and our interest in finding a method for determining the relative amounts of the MCP and OCP in deformed bulk samples, which is independent of the orientations of the phases in them, provided a convenient opportunity for undertaking the present study.

It is not our intention to dwell in any detail in this paper on how mechanical deformation leads to the occurrence of the MCP. Aspects of this problem have been considered in several papers in which various possible modes of crystal–crystal transformation from the orthorhombic to the monoclinic crystalline forms of polyethylene have been discussed[6,8-13,15]. While as indicated earlier, our main concern in this paper is to illustrate the application of ^{13}C n.m.r. for assessing the ratio of the MCP to OCP in strained polyethylene, we will also describe some results derived from additional n.m.r. experiments which bear on the proximities of the OCP, MCP and NC regions relative to one another, as well as on the orientation of the chains in the NC regions relative to the stretching direction.

EXPERIMENTAL

Ultra high molecular weight polyethylene specimens (UHMWPE)

Compression moulded sheets of UHMWPE were made from Hercules 1900 UHMW[30] polymer (Batch No. 90452, $M_w \approx 4 \times 10^6$). The morphology of the raw polymer particles, details of the moulding conditions, and aspects of the structure and morphology of the as-moulded and stretched sheets, as well as aspects of the mechanical properties of the sheets have been reported elsewhere[27-29]. We confine ourselves here to a summary of features pertinent to the present study.

The sheets of UHMWPE were moulded as follows[27]. The raw polymer contained in a mould under vacuum was heated slowly in a press to 200°C. After 10 min at 200°C a pressure of 8.25 MPa was applied to the molten polymer. The mould was then allowed to cool to room temperature (the rate of cooling between 200°C and 100°C was approximately 1°C min^{-1}). The sheets were approximately 1.0 mm thick and their density as measured in an ethanol/water density gradient column at 23°C was in the range 0.934–0.936 g cm^{-3} (weight % crystallinity 58%–60% based on a crystal density of 1.0 g cm^{-3} and an amorphous density of 0.855 g cm^{-3})[27]. The effect of uniaxial stretching at room temperature on the compression moulded samples of UHMWPE is characterized by two main features[27]. First, in contrast to the stretching behaviour of lower molecular weight polyethylene (e.g. $M_w = 10^4$–10^5) the UHMWPE specimens do not exhibit macroscopic necking even up to the point of fracture (which occurs at a strain of approximately 4 for a strain rate of ≈ 0.02 min^{-1}). Second, the stretched specimens exhibit considerable recovery from the imposed stretching when they are released under zero stress. As expected the residual strains in the released samples were larger the greater the initial stretching; they ranged from 0.05–1.72 for samples which were stretched to strains in the range 0.25 to 3.0[28].

The strained specimens used in the present study were prepared as follows: Dumbbell shaped specimens 7.5 cm in overall length were stamped out from the undeformed moulded sheets. The narrow gauge region was 3 cm × 3 mm. These specimens were initially stretched at room temperature uniaxially in an Instron machine[30] to a strain of 3.0 (measured in the narrow gauge region) at a rate of 1.0 mm min^{-1}. They were then immediately released under zero stress whereupon they contracted. The residual longitudinal strain in the narrow guage part of the specimens after 24 h was 1.69. Further shrinkage was not monitored. However (based on longer term shrinkage measurements on other samples), it could be estimated that the residual strain in the specimens was approx. 1.5 at the time that the n.m.r. and X-ray diffraction data described in this paper were obtained. We shall refer to undeformed and deformed specimens (stretched/released, residual strain 1.5) as UDPE and DPE, respectively, in the remainder or this paper.

Wide-angle X-ray diffraction patterns of UDPE and DPE specimens are shown in *Figure 1* and *Figure 2*, respectively. These patterns were recorded with a flate plate camera using nickel filtered CuK_α radiation. The following distinguishing features of the most intense X-ray reflections characteristic of the OCP and the MCP serve as background for the ensuing description of these diffraction patterns. The suffixes (*o*) and (*m*) are used to differentiate between the indices of reflections from the two structures. The strongest orthorhombic reflections are the 110_o and 200_o whose corresponding spacings are 0.41 mm and 0.37 mm[16], whereas the spacings of the strongest reflections of the metastable phase are 0.458 nm, 0.380 nm and 0.355 mm[5,7,8]. In terms of the monoclinic

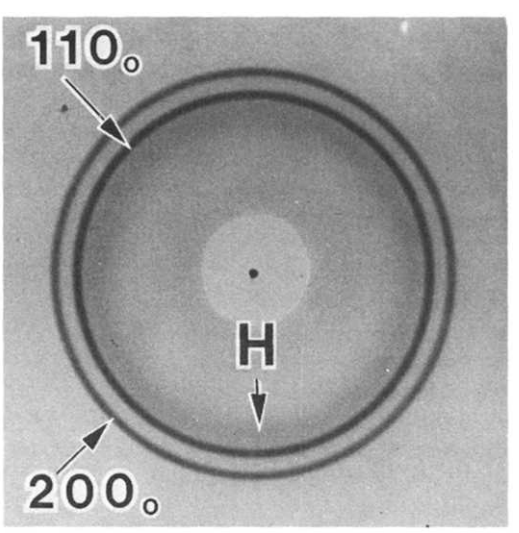

Figure 1 Wide-angle X-ray diffraction pattern of an undrawn (UDPE) compression moalded specimen of UHMWPE showing the characteristic 110_o and 200_o diffraction rings of the orthorhombic crystal phase[16], and the diffuse halo H due to the non-crystalline regions

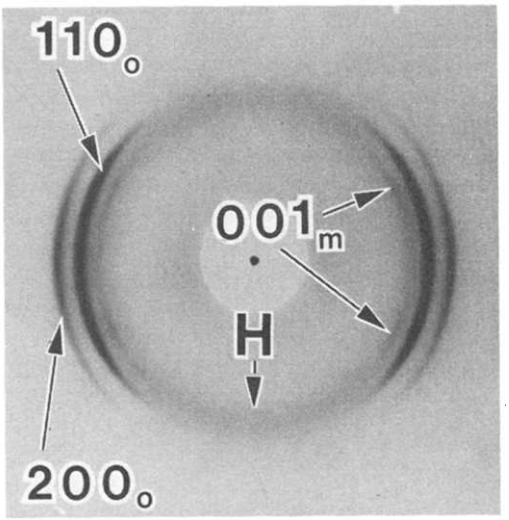

Figure 2 Wide angle X-ray diffraction pattern of a specimen of compression moulded UHMWPE which was stretched uniaxially to a strain of 3.0 and then released and allowed to contract under zero tension; the residual strain in the sample (DPE) was 1.5. 001_m arcs due to the monoclinic crystal phase may be seen in addition to the much more intense 110_o and 200_o arcs of the orthorhombic phase. Stretching direction is vertical

cell of Seto *et al.*[8] ($a=0.809$ nm, $b=0.253$ nm, $c=0.479$ nm, $\beta=107.9°$), the indices of these latter three reflections are 001_m, 200_m and 201_m, respectively, among which the first (spacing 0.45–0.46 mm) is usually observed to be the most intense of the three. It should be noted that the chains in the unit cell of Seto *et al.*[8] are parallel to the *b*-axis. We emphasize that feature to avoid any confusion arising from different assignments of the cell parameters which have appeared in the literature, e.g. ref. 31. (In the same vein we point out that the indices of three MCP reflections expressed in terms of the triclinic cell proposed by Turner-Jones[7] are 010_t, 100_t and $1\bar{1}0_t$, respectively).

The UDPE X-ray diffraction pattern in *Figure 1* exhibits the intense 110_o and 200_o diffraction rings characteristic of the OCP. A broad diffuse inner halo (H) due to the amorphous or non-crystalline regions is also evident in that pattern in which there is no detectable evidence of any MCP reflections.

In the pattern of the DPE specimen (residual strain 1.5) in *Figure 2* the orthorhombic 110_o and 200_o reflections occur as arcs spread azimuthally about the equator. An inner diffuse halo (H) due to the NC regions can also be seen. *In addition*, however, relatively weak but sharp arcs, corresponding to a spacing of 0.456 and which are superimposed on the diffuse inner halo (H), are present in the pattern. These 001_m arcs overlap at the equator but are split about it. They are centred on azimuthal axes oriented at approximately $\pm 65°$ to the direction of tensile deformation. The 200_m and $\bar{2}01_m$ reflections of the MCP are not discernible in *Figure 2*. They could be seen, however, as faint arcs spread about the equator in 'overexposed' diffraction patterns.

The n.m.r. study reported in this paper is limited to the UDPE and DPE samples described above. It is of interest, however, in anticipation of any future more detailed studies of the partially reversible deformation processes exhibited by UHMW polyethylene, to mention three additional observations concerning the occurrence of the MCP in strained samples. First, wide-angle X-ray diffraction patterns of all samples with residual strains in the range 0.2–1.7 exhibited the presence of a small fraction of MCP. As is the case in *Figure 2* the MCP reflections were considerably less intense than those of the OCP. Second, MCP reflections were also observed in diffraction patterns of samples which had been stretched and kept under tension at constant strain[29]. Third, the intensities of the MCP reflections decrease considerably relative to the OCP when initially stretched samples were subsequently released and allowed to contract[29]. A similar decrease in MCP relative to OCP content upon removal of external stresses has been previously observed in the case of lower molecular weight polyethylene[3,8].

Evidently, the manifestation of polymorphism associated with the partially reversible deformation characteristics of UHMWPE summarized above is but one aspect of the effects of deformation on the polymer. Detailed elucidation of the processes involved in its mechanical deformation requires the determination of the corresponding changes in fine texture at different strains both during stretching and after subsequent contraction under zero stress. This is beyond the scope of the present investigation. However, as additional background for any such detailed studies in the future, we summarize below some qualitative observations (based on small-angle X-ray diffraction) concerning the nature of the fine textures of the UDPE and DPE samples used in the present n.m.r. investigation.

SAXD patterns of the UDPE and DPE specimens were recorded photographically with a Rigaku–Denki small angle camera using pinhole collimation and nickel filtered CuK_α radiation. No discrete diffraction ring was discernible in the SAXD pattern of the UDPE specimen. This suggests two possibilities. Either the lamellae in the compression moulded UDPE are thicker than approximately 40 nm which was the upper limit of the periodic fine structural detail resolvable under the prevailing experimental set-up, or there is a broad distribution in the thickness of the lamellae in the specimen because the moulded samples were not crystallized isothermally. The DPE specimen exhibited a 'tilted four-lobed' SAXD pattern, an example of which is shown in *Figure 3*. Four diffuse off-equatorial lobes with their long axis inclined at $\approx 25°$ to the equator can be readily seen in this Figure. Furthermore, the disposition of the lobes is not radial, i.e. the long axis of each lobe does not point to the centre of the pattern. In addition to these features it can be seen that the diffuse central scattering in *Figure 3* is streaked equatorially suggesting that the fine texture of the DPE

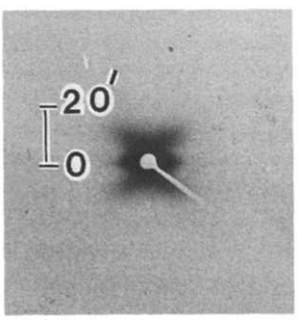

Figure 3 Small angle X-ray diffraction pattern of the same deformed specimen (DPE) as that of *Figure 2*. Stretching direction vertical. (Scale indicates Bragg angle θ' corresponding to distance from the center of the pattern)

specimen is fibrillar in character with the possible presence of elongated voids oriented with their longer axis parallel to the stretching direction. While the occurrence of the aforementioned tilted off-equatorial lobes points to an alternation of ordered (crystalline) and disordered (NC) regions along paths parallel to the stretching direction[32-34]; it was not possible to derive directly by simple inspection of the photographically recorded SAXD pattern, any estimate of a periodicity in the fine texture in that direction, as would have been possible, for example, in the case of a simple four-pointed pattern. We point out in this connection the diffuse nature of the lobes and the absence of any evident intensity maximum in each. The four-lobed character of the off equatorial scattering suggests that the interfaces between alternating ordered and disordered regions in the direction of stretching may not be orthogonal to that direction. We have not attempted to analyse the SAXD characteristics of the DPE sample any further. A basis for future quantitative analyses aimed at characterizing the fine structure of the DPE specimen is provided by models previously proposed to account for four-lobed SAXD patterns exhibited by deformed specimens of lower molecular weight polyethylenes[33,34]. A discussion of these models is beyond the scope of the present paper.

N.m.r. measurements

The n.m.r. measurements were carried out using two spectrometers, a non-commercial spectrometer operating at a field of 1.4T (15.08 MHz for ^{13}C) and a commercial spectrometer (Bruker CXP-200)[30] which operates at a field of 4.7T (50.3 MHz for ^{13}C). Magnetization was generated by spin-lock cross polarization[35,36] (CP) from the protons. Samples were spun at the 'magic angle' in order to eliminate anisotropic chemical shift broadening[37,38]. Rotational frequencies (RF) were approximately 2700 and 1900 Hz at 4.7T and 1.4T, respectively. The ^{13}C-signals were observed at ambient temperature in the presence of high-power proton decoupling. The proton RF field strength was 50 KHz at 4.7T and 60 KHz at 1.4T; the ^{13}C RF fields were matched[35] to the proton RF fields at values which differed by approximately the spinning speed in order to provide maximum polarization transfer efficiency between the protons and carbons during cross-polarization[39]. Generally, a 1.5–2.0 ms CP time, t_{cp}, was used. Phase alternation was also employed to minimize baseline artifacts[40]. A deuterated polymethylmethacrylate (PMMA) rotor was used to house the samples at 4.7T while at 1.4T, polychlorotrifluoroethylene was used.

The UDPE sample was loaded into the rotor as a stack of rectangular plates. The DPE sample was made up of 7 mm lengths cut from six different dumbbells in the regions where the strain as 1.5. The lengths were stacked parallel to the rotation axis. The non-spinning sample used for studying orientation in the DPE consisted of the 7 mm lengths aligned parallel to one another and placed in a rectangular window cut into a Teflon cylinder in a transverse direction.

A discussion of the n.m.r. RF pulse sequences used, along with their rationale, is presented at the end of the next section.

BACKGROUND OF N.M.R. MEASUREMENTS

Quantitative aspects of cross-polarization spectra

The ^{13}C signals arising from undisturbed Boltzmann equilibrium populations have rigorously quantitative relative intensities. However, a sensitivity problem exists when attempting to measure this population directly because signal averaging to improve signal-to-noise requires delay times between experiments of a few thousand seconds since longitudinal ^{13}C relaxation times, T_1^C are of the order of 300–4000 s for carbons in the crystalline region[41,42] of polyethylene. On the other hand, repetition times for signal averaging using CP techniques depend on *proton* relaxation times, T_1^H, which are generally of the order of 1 s at room temperature due to proton spin diffusion[43,44]. (The phenomenon of spin diffusion is analogous to heat induction in a heterogeneous system; spin diffusion is discussed in more detail in the next section.) Thus, if one is looking for signals representing a component present at the level of a few per cent as in the present case, the CP technique is dictated because of its higher sensitivity. Moreover, there is a fourfold theoretical sensitivity enhancement factor[36] associated with the CP method compared to the former technique. In exchange for the sensitivity advantage, the possibility arises that the CP technique may not be quantitative. This point is therefore considered further below.

True relative intensities and near theoretical enhancement factors are obtained when the following three criteria are satisfied: (a) the cross-polarization times are short compared with the shortest proton rotating framd relaxation time, T_ρ^H (min), (b) the proton RF field is much larger than the local proton–proton dipolar fields, and (c) cross-polarization time constants, T_{CH}, are short enough to allow the ^{13}C nuclei to 'equilibrate' with the protons during the cross-polarization period. A detailed discussion of these criteria is beyond the scope of this paper; however, a couple of general comments are in order. If molecular motion lies in the midkilohertz range, then $T_{1\rho}^H$ becomes short (as short as 10^{-4} s) thus challenging the validity of criterion (a) above. With RF field strengths of 50–60 KHz criterion (b) creates signal variations of only a few per cent throughout the polyethylene sample[45]. Finally, if there are regions of a sample where molecular motion is nearly isotropic and where resulting proton linewidths are small, the CP process becomes very inefficient compared to the rigid solid so that satisfaction of criterion (c) becomes questionable.

In polyethylene we have found that the CP enhancement factor varies. For the crystalline regions it is relatively constant at 3.5 ± 0.2, while in the NC regions it is more sample dependent, ranging between 2.4 and 3.0. These values are typical for CP times in the range of 0.7–2.0 ms. The crystalline enhancement factors cited have uncertainties which reflect the poor signal-to-noise ratio in the determination of the corresponding equilibrium signal; the range given for the NC enhancement represents real differences since the equilibrium NC signal can be determined easily by pulse sequences which repeat at rates of 5–10 s and which are chosen to avoid transient Overhauser effects[46]. (By way of clarification, a typical T_1^C decay curve in polyethylene yields three components, only one of which has a T_1^C less than 1 2. It is this latter component which comprises the major portion of what we refer to herein as the NC ^{13}C signal and which

corresponds to the NC enhancements given. For the purposes of this paper we will continue to refer to a single NC region). The source of the smaller NC enhancement factor in polyethylene relative to that of the crystal is due to a combination of criteria (a) and (c) above not being rigorously fulfilled because molecular motion shortens $T_{1\rho}^{H}$ and lengthens T_{CH} in the NC region.

Since CP spectra of polyethylene will contain intensity distortions between the NC and crystalline signals, we turn to the more critical concern, namely, possible intensity distortions of the MCP signal relative to the OCP signal. In principal, since both of these phases are crystalline and since the molecules in the OCP (and probably also the MCP) have very limited mobility at ambient temperature, the intrinsic $T_{1\rho}^{H}$'s of these phases are expected to be long enough to satisfy criterion (a) above. Moreover, the characteristic time, T_{CH}, describing proton–carbon equilibration during CP is expected to be less than 0.13 ms for a rigid methylene group in a proton-rich environment[47]. Therefore, considering only the isolated crystalline regions, it is straightforward to satisfy criteria (a)–(c) above and expect quantitative relative intensities for the OCP and MCP signals. Any question concerning the quantitative character of the relative OCP and MCP signals in the CP spectra thus boils down to the way in which the NC spin dynamics influence the OCP and MCP signals.

The mechanism of influence is spin diffusion between the NC and crystalline phases which may distort relative intensities when corresponding differences in relaxation behaviour exist. Since the importance of spin diffusion is related to morphology, any characteristic differences in proximity to the NC region could, in principle, give rise to relative intensity distortions of the OCP and MCP signals.

Since spin-diffusion, which is discussed more fully in the next section, requires a magnetization gradient, the mechanism for generating this gradient must exist. This mechanism in the CP experiment is a difference in the intrinsic $T_{1\rho}^{H}$ values between the NC and crystalline regions. Obviously then, if all $T_{1\rho}^{H}$'s are much longer than T_{CP}, which in turn should be at least as long as, say, $5T_{CH}$ ($5T_{CH} < 700\ \mu s$ for the crystalline carbons of polyethylene) then the influence of spin diffusion will be negligible in its ability to distort the true relative intensities of the OCP and MCP signals. Therefore, establishing favourable $T_{1\rho}^{H}$ values might well establish quantitative relative intensities for the OCP and the MCP and avoid the necessity of characterizing the spin diffusion behaviour.

In this paper, we have elected to look into both the $T_{1\rho}^{H}$ behaviour as well as the spin-diffusion behaviour in the UDPE and DPE samples. The aspect of spin diffusion was pursued in part because it is relevant to the quantitation question (but in view of the $T_{1\rho}^{H}$ values was not critical to this question), and in part because some additional qualitative insight concerning NC proximities to the OCP and MCP could be obtained.

Spin-exchange and spin-diffusion

It is a characteristic of dipolar interactions between like nuclei that spin exchange occurs, provided other local spin perturbations (e.g. quadrupolar, chemical shift or nucleus-unpaired-electron interactions) are absent or at least smaller than the dipole–dipole interactions.

A useful investigation of spin-exchange in n-alkanes has been published by Douglass and Jones[44]. Their paper contains a formalism for describing the associated phenomenon of 'spin-diffusion', i.e. the transport of (proton) magnetizations; furthermore, estimates are given for spin diffusion constants in n-alkanes.

The key concept is that spin-diffusion is a mechanism for *transporting proton magnetization* from one region to another in a heterogeneous system. Thus if the heterogeneous system has heterogeneous relaxation behaviour as well, one ought to be able to design experiments where signals near the boundary of a domain are enhanced (or suppressed) relative to the interior of that region.

Since the conclusions based on spin-diffusion experiments in the present paper are qualitative, only a few relevant comments will be made. First, spin diffusion, in a strong static magnetic field, proceeds both in the presence and in the absence of strong resonant proton RF fields. The only difference between these two cases is that the term in the dipolar Hamiltonian which is responsible for spin exchange is twice as big in the absence of the RF field as it is when a resonant field (50–60 KHz in strength) is present. Therefore each corresponding diffusion constant, describing magnetization transport, will differ by this same factor of two. Thus, spin diffusion must be taken into account in both T_1^{H} and $T_{1\rho}^{H}$ measurements.

Second, the magnitude of the diffusion constant, D, in the alkanes was estimated[44] to be 6.2×10^{-12} cm^2 s^{-1} in the absence of a proton RF field. In the alkanes, a one-dimensional description of the diffusion process is appropriate and from the theory one may calculate typical distances, $x(t)$, over which magnetization diffuses in a given time. Roughly speaking, the propagation of a magnetization 'front', starting at $x=0$ at $t=0$ and penetrating an infinite medium is described by the relationship[48]

$$x^2(t) = 4Dt \tag{1}$$

whereas the realtionship

$$x^2(t) = 2Dt \tag{2}$$

describes a similar situation in a finite medium where gradients between $x=0$ and $x(t)$ are no longer very significant[49]. Using equation (1) and the value of D above, values for $x(t)$ 1.6, 7.0 and 50 nm correspond to times of 1 ms, 20 ms and 1 s, respectively. Thus, for example, suppose that one wished to enhance crystalline resonances from those parts of the crystalline regions of polyethylene which lie near the NC boundaries. Further, suppose that the crystal thickness is 15 nm and that one can quickly prepare only NC proton magnetization. Then, in order to maintain a reasonable magnetization gradient across the crystalline region, diffusion times should be limited to approximately 20 ms. For times in the order of 20 ms, there is some contribution from interior resonances but the signal intensity would still be significantly weighted towards carbons near the NC surface.

A final remark about spin diffusion is that magic angle spinning (MAS), when fast enough, can interfere with the spin diffusion process and slow it down[50]. This phenomenon is also associated with a narrowing of the dipolar broadened resonance lines in homonuclear systems when the spinning frequency approaches the linewidth; simul-

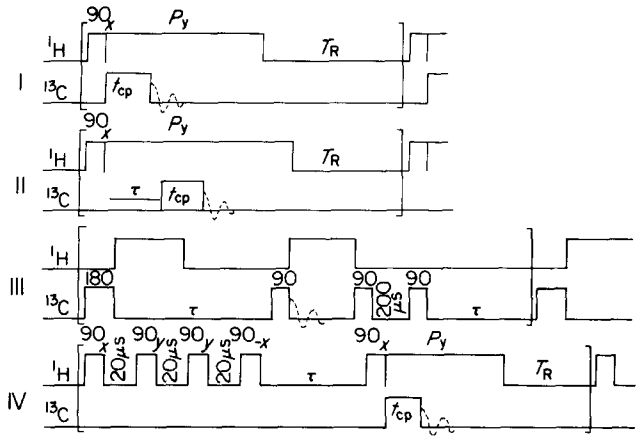

Figure 4 Experimental *rf* pulse sequences employed in this work. Nomenclature is as follows: ^{1}H and ^{13}C refer to the nuclei irradiated by the *rf* pulses; numbers such as 90 or 180 refer to a pulse of appropriately chosen length to produce a nuclear nutation of the indicated number of degrees; subscripts refer to the relative *rf* phases of different pulses using the convention that *y* and *-x* respectively have phase differences of 90° and 180° with respect to the *x* phase; p_i refers to a pulse of unspecified duration (usually several ms) having phase *i*; t_{cp} is the cross polarization time and T_R is the delay time between experiments. Dashed-lines decays are shown at points of signal observation. Sequence I is the usual cross-polarization (CP) sequence; Sequence II measures proton rotating frame relaxation indirectly via ^{13}C signals; Sequence III is a sequence for selectively observing the non-crystalline ^{13}C signals in polyethylene while suppressing the crystalline signals. Extra pulses are added to insure ^{13}C saturation after observation and to suppress transient Overhauser distortions for the long relaxing (crystalline) carbons. Sequence IV selects only NC proton magnetization in the first four pulses, storing this magnetization along the static magnetic field. Then, after a time, τ, a ^{13}C signal is generated via CP and in this way, spin diffusion from the NC to the crystalline regions is monitored

taneously spinning sidebands appear in the spectra. All spinning speeds used here were small compared to crystalline proton linewidths; therefore, no effect of MAS is expected on the crystalline diffusion constant, D_C. For the non-crystalline diffusion constant, D_{NC}, some rotational-speed dependence might be expected for spinning frequencies, ν_r, above 2.0 KHz since this is the frequency at which spinning sidebands in the proton spectrum first become visible[51]. Therefore, results obtained at 1.4 T at $\nu_r = 1900$ Hz are emphasized in this paper over the results obtained at 50 MHz and $\nu_r = 2750$ Hz.

Pulse sequences and their rationale

The RF pulse sequences used to obtain the n.m.r. spectra are shown in *Figure 4*. The conventions and nomenclature defining the pulses and their relative phases are defined in the Figure captions. Sequence **I** is the basic spin-lock cross-polarization (CP) sequence[36]. Sequence **II** is a sequence which discriminates strongly against carbons in regions where attached protons have rotating frame-relaxation times, $T_{1\rho}^H$, less than τ. Sequence **III** has been used previously to isolate NC resonances quantitatively in polyethylene[52]. The two 90° carbon pulses following observation ensure saturation of the ^{13}C signal. The proton pulse following the 180° carbon pulse helps to minimize the contribution to the observed signal from the transient Overhauser effect[46] for carbons with long T_1^C's. When τ is chosen to be 10 s, sequence **III** yields numbers which, we have found, agree very well with d.s.c. and density determinations of the NC content.

Sequence **IV** monitors spin diffusion. The objective is to establish initially non-crystalline proton magnetization only (along $\underline{B}_0$) in a time short enough so that spin-diffusion between the crystalline and non-crystalline regions can be neglected. Following this preparation period, there is a variable period, τ, during which magnetization diffuses from the non-crystalline into the crystalline regions. At very early times in this diffusion process, the crystalline magnetization so generated, will be relatively weak in signals arising from carbons in the interior of the crystallites. At the end of the τ period, the status of the proton magnetization is monitored via CP. In practice, the first four proton pulses of sequence **IV** reestablish, in a time of 76 μs, approximately 60% of the original non-crystalline proton magnetization along $\underline{B}_o$. At the same time, the crystalline magnetization is attenuated to less than 1% of its original value. This four-pulse sequence was arrived at in a semiempirical fashion. Roughly, the sequence combines the discriminating ability of the free induction decay (different proton T_2's) and the pulse-spacing dependence of the solid echo[53,54] for preserving magnetization associated with the narrower portion of a resonance line. The objective for sequence **IV** parallels that of the Goldman–Shen experiment[55]; the differences arise because of the indirect readout of the proton magnetization via CP and because the first four pulses of sequence **IV** were found to preserve more non-crystalline proton magnetization than the Goldman–Shen experiment does, given the differences in proton T_2's in the respective phases of the polyethylene samples investigated and the desired level of suppression of crystalline magnetization.

A combination (not shown) of sequences **II** and **IV** was used to measure $NC_{1\rho}^H$'s. The fourth 90° proton pulse of sequence **IV** was replaced by a long spin-locking pulse of duration τ prior to CP and observation as in sequence **II**.

N.M.R. RESULTS

Quantitation of relative intensities

Figure 5 shows spectra taken at 1.4T of the undrawn (UDPE) and the drawn (DPE) samples of the ultrahigh molecular weight polyethylene. Spectra 5A–5C and 5D–5F refer to the UDPE and DPE samples, respectively. Spectra 5A and 5D are the ^{13}C CP–MAS spectra taken with sequence **I**. Spectra 5C and 5F were taken with sequence **III** and represent non-crystalline lineshapes. Spectra 5B and 5E are difference spectra (5B = 5A − 5C; 5E = 5D − 5F) representing the pure crystalline lineshapes. The existence of the MCP is clearly demonstrated in the sharp peak at 35.0 ppm in spectra 5D and 5E. This peak is shifted 1.4 ppm downfield from the OCP peak. Moreover, consistent with the wide-angle diffraction observations, spectra 5A and 5D of the UDPE sample do not exhibit this MCP resonance. Spectra 5A and 5D are normalized to the same total intensity while the intensities of 5C and 5F have been adjusted to give spectra 5B and 5E. The crystalline linewidths are 6.5 Hz in the DPE spectra and 9.0 Hz in the UDPE spectra. From the observed relative intensities obtained using sequences **I** and **III** in the two samples average CP enhancement factors for the non-crystalline (NC) signals can be ob-

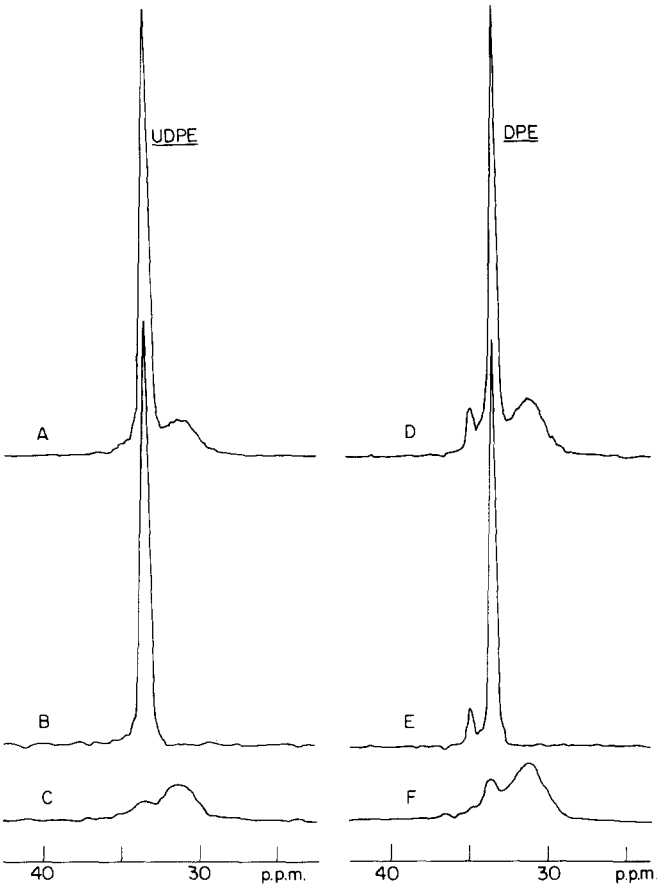

Figure 5 15.08 MHz ^{13}C magic-angle spinning (MAS) spectra of UHMWPE the undrawn (UDPE) and drawn (DPE) UHMWPE samples. Spectra A and D are CP spectra (Sequence I of *Figure 4*, t_{CP}=2ms); Spectra C and F are the NC signals (Sequence III of *Figure 4*, τ=10s); Spectra B and E are differance signals (B=A-C; E=D-F) which represent the pure crystalline signals. Note the MCP signal downfield from the OCP in spectra D and E. Spectra A and D are normalized to the same total intensity, spectra C and F are adjusted to eliminate the NC signals in Spectra B and E

tained. They are 2.4 and 2.9 for the UDPE and DPE samples respectively after a 2 ms CP time.

Since we know the true ratios of crystalline to NC signals in the two samples from the enhancement factors and the non-crystalline lineshapes, the weight fraction crystallinity, f_c, can be determined if we assume that the crystalline enhancement factor is 3.5 ± 0.2. For the UDPE and DPE samples, f_c is 0.59 ± 0.2 and 0.46 ± 0.03, respectively. These determinations include the subtraction of that part ($\approx 6\%$) of the lineshape intensity of spectra 5C and 5F which has the corresponding crystalline lineshape. The value of f_c for the UDPE sample is in excellent agreement with the weight fraction crystallinity, 0.59, obtained from density measurements (see Experimental). No density measurements were taken on the DPE sample because of complications due to voids.

Having established the crystalline fractions in these samples we turn to the question of the quantitative relative intensities of the OCP and the MC signals in the CP spectra. As discussed in the previous section, a sufficient condition for these intensities to be quantitative is that all $T_{1\rho}^H$'s be sufficiently long relative to an appropriate t_{cp}. The measured NC $T_{1\rho}^H$ values were 8 ms and 13 ms while the crystalline $T_{1\rho}^H$ values were 170 and 65 ms, respectively, for the UDPE and DPE samples. Since the UDPE showed no identifiable MCP, only the DPE sample will be considered. From the NC and crystalline $T_{1\rho}^H$ values and their ratio one can estimate that the maximum decrease in crystalline intensity due to spin diffusion from the crystalline region to the NC regions is a few per cent over a t_{cp} of 2 ms. Thus, unless there is some very substantial morphological difference in the sites occupied by the MCP and the OCP such that spin-diffusion preferentially couples to one of the two phases, the relative intensities of the OCP and MCP signals in *Figures 5D* and *5E* ought to represent the true relative weight per cents of these phases in the DPE sample.

Two experiments were performed in an effort to determine whether significant morphological differences exist between the MCP and OCP of the DPE which could give rise to any such relative intensity distortions. The first experiment (sequence **II**) simply monitored the MCP to OCP relative intensity at a t_{cp} of 2 ms using a variable proton spin-locking preparation period, τ. The results are illustrated in *Figure 6* (Details are explained in the caption.) The changing ratios of the crystalline and NC signals in spectra 6A and 6C coupled with the unchanged (within experimental error) ratios of the MCP to the OCP in spectra 6B and 6D indicate that if spin diffusion between the NC and crystalline regions determines the $T_{1\rho}^H$ of the crystalline phases, then the two crystalline phases seem to have similar proximities to the NC regions. Although the importance of a spin-diffusion connection between the NC and the crystalline regions is not verified in *Figure 6*, (the MCP and the OCP could be isolated from

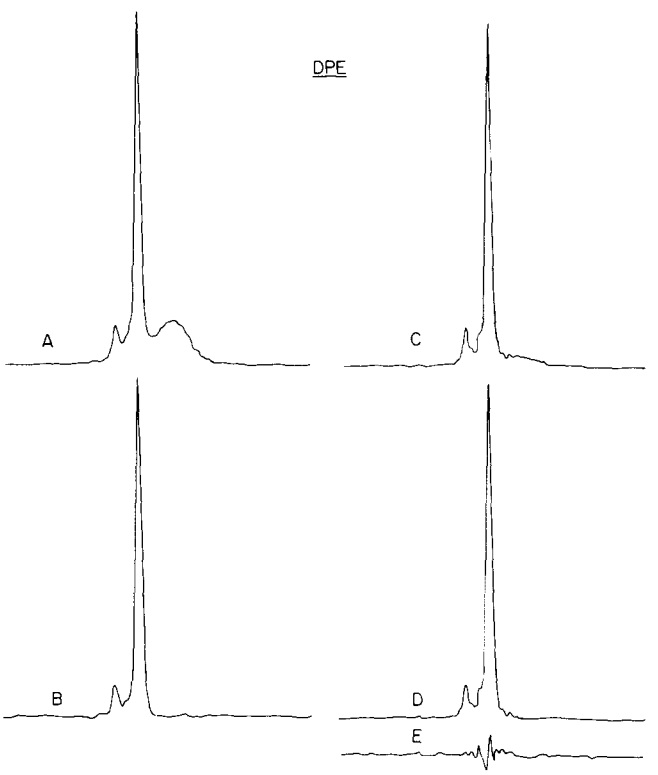

Figure 6 Demonstration of the constant MCP/OCP signal intensity ratio as a function of proton spin locking time using Sequence II of *Figure 4*. These are ^{13}C MAS spectra at 15.08 MHz. Spectrum A: τ=100μs, t_{cp}=1ms; spectrum B: same as spectrum 5E; spectrum C: τ=40ms, t_{cp}=1ms; spectrum D is spectrum C with the removal of the NC signal using spectrum 5F; spectrum E=B-D. Spectrum C has been normalized in intensity so as to match crystalline signal amplitudes in A and C. The NC signal is about 25% as large in C as in A in this display

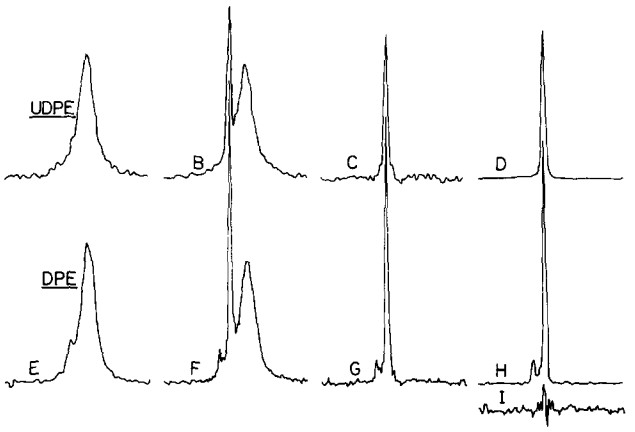

Figure 7 15.08 MHz ^{13}C MAS spectra taken using sequence IV of *Figure 4*. Spectra A–D refer to the UDPE sample and E–I refer to the DPE sample. Spectra A and D have $\tau = 100\,\mu s$, $t_{cp} = 0.5$ ms; Spectra B and F have $\tau = 19$ ms, $t_{cp} = 0.5$ ms; spectrum C = B-O; spectrum G = F-0.85. Spectrum D and H are scaled versions of spectra 5B and 5E and are normalized to be equal to the intensities in spectra C and G respectively. Spectrum I = G-H. Spectra A and E are normalized to be same intensity. The similar ratios of MCP to OCP intensities in spectra G and H indicate that the average distance from MCP protons to the nearest NC protons is the same as the average distance from OCP protons to their nearest NC protons

the NC regions and yet have the same $T_{1\rho}^{H}$) the quantitative character of the OCP and MCP relative intensities is established, whether or not spin diffusion is the mechanism for crystalline $T_{1\rho}^{H}$ relaxation. Accordingly, analysis of spectrum 5E then indicates that the DPE sample contains $8.5 \pm 1\%$ MCP relative to the total crystalline content.

In the second experiment aimed at exposing possible morphological differences between the MCP and OCP environments sequence **IV** was used and some results are illustrated in *Figure 7*. Details of each spectrum are again given in the Figure caption. In this experiment spin-diffusion should be twice as strong (laboratory frame) as in the previous experiment (rotating frame). Any spin-diffusion quenching effects resulting from the magic-angle spinning should therefore also be less effective. Although it is realized that the results of *Figure 7* are not needed in order to establish the quantitative relative intensities of the OCP and the MCP signals, these results are presented because they reconfirm the quantitative relative intensities of the OCP and MCP signals while giving a more direct indication of the importance of spin diffusion, thereby also providing some morphological information. Since many of the deductions from the results of *Figure 7* are peripheral to the question of quantitative relative intensities, only summarizing statements will be made:

(a) The growth of crystalline magnetization at $\tau = 19$ ms in spectra 7B and 7F is due to spin diffusion from the NC region because the NC intensities are reduced relative to the corresponding spectra at $\tau = 100\,\mu s$. Further support for this claim can be argued by recognizing that the growth of significant crystalline proton intensity during τ via intrinsic proton T_1 processes is unlikely because very few if any crystalline carbons have short T_1's (see spectra 5C and 5F).

(b) The rate of growth of crystalline magnetization via spin diffusion in sequence **IV** is approximately consistent with the idea that crystalline $T_{1\rho}^{H}$ values are determined by spin-diffusion assuming that magic angle spinning at the speeds used does not appreciably quench spin diffusion in the rotating frame.

(c) The near absence of a crystalline signal in spectra 7A and 7E ($\tau = 100\,\mu s$, $t_{cp} = 0.5$ ms) suggests that in the normal CP experiment with $t_{cp} = 2$ ms, spin-diffusion between the crystalline and NC regions perturbs the crystalline intensities at levels no larger than 2%, thus strongly reinforcing the quantitative claims established earlier. However, this weak apparent spin-diffusion in the rotating frame during t_{cp} might also be partially traced to some additional spatial selection of magnetization within the NC region by the four-pulse preparation of sequence **IV**. Thus, the weakness of NC to crystalline spin-diffusion is confirmed but its magnitude may still be a few per cent rather than limited to 2% over 2 ms.

(d) The similarity in the line shapes in spectra 7G and 7H (see spectrum 7I) imply that spin-diffusion, at the relatively short time of 19 ms, has populated the MCP and the OCP to the same extent in the DPE. This, in turn, implies that both crystalline phases have the same average proximity to the NC regions. However, the latter statement applies only if a significant magnetization gradient exists across the crystalline regions after 19 ms. Using the relationships given in equation (1), a one-dimensional diffusion model, and a D of 6.2×10^{-12} cm^2 s^{-1}, one may claim the existence of a significant gradient when the average crystal dimension between nearest NC boundaries, L_m, exceeds 14 nm. Since it was not the original intent to study crystallite dimensions, and since periodicities cannot be easily inferred from the SAXS pattern, only the following qualified conclusion can be set forth, i.e. *if* the minimum crystal dimension between NC boundaries is on average greater than 14 nm, then the MCP and OCP crystalline regions show similar such dimensions. This conclusion will be referred to as the NC proximity conclusion. In this connection, computer modelling studies[49] of spin-diffusion during spin-locking have suggested that this dimension may be estimated from the crystalline $T_{1\rho}^{H}$ value through the relationship $L_m^2 = 8 D_r T_{1\rho}^{H}$ where D_r is the rotating frame diffusion constant ($= 3.1 \times 10^{-12}$ cm^2 s^{-1}). This relationship gives $L_m = 13$ nm in DPE which is very close to the required 14 nm. Thus, it is likely that similar dimensions, L_m, do prevail in the MCP and the OCP. Indeed this is expected from the proposed mechanisms of crystal–crystal transformation giving rise to the MCP[6,8–13,15]. The n.m.r. evidence simply adds the point that there is no significant size selection in the crystallites which are transformed.

(e) Comparison of the rates of crystalline magnetization growth during τ in *Figure 7* indicates that given a magnetization gradient between the crystalline and NC regions spin-diffusion transports magnetization twice as fast, on a weight basis, in the DPE sample relative to the UDPE sample. Since the propagation of magnetization at early times is proportional[56] to the surface area multiplied by $D^{1/2}$, an increase (a maximum twofold increase) in surface area and/or an increase in the NC diffusion constant could be responsible for the observed difference in rates. Direct observation of proton NC linewidths indicate that NC linewidths are 4.4 and 9.0 KHz in the UDPE and the DPE samples respectively. Since most of the molecular motions in the NC regions of polyethylene at ambient temperatures are high frequency[57] compared to the frequency of the dipolar interactions, it is reason-

able to suppose that the NC diffusion constants are proportional to the NC linewidths[58]. Of course magic angle spinning could also preferentially quench spin diffusion in the UDPE relative to the DPE. The possibility of quenching was only tested in the DPE sample where it was found that varying the spinning frequency between 1400 and 2800 Hz did not affect the transfer rate. However, until the effects of magic angle spinning on spin diffusion rates in UDPE are evaluated, one cannot estimate the changes in crystal/NC surface area with precision.

Orientation measurements

In UHMWPE, a sample under extensional loading exhibits a higher MCP content than when it is released under zero tension and is allowed to shink (see Experimental). Moreover some wide-angle X-ray diffraction experiments on UHMWPE indicate that for two specimens having the same strain (e.g. 0.4) one of which was stretched and kept at that strain under tension, while the other was allowed to contract under zero stress from a larger strain (1.0), the MCP content in the former was higher. These observations indicate that the formation of the MCP upon stretching is partially reversible and that it is stabilized by the presence of external stresses. This suggests that the MCP present in stretched specimens after they are allowed to contract under zero stress may be stabilized by *internal* stresses. A possible feature which might correlate with internal stresses is the orientation of chains in the NC region. Since the NC signals can be separated using sequence **III**, and since non-spinning spectra are sensitive to orientation[59], it was decided to measure orientation in the DPE sample.

Figure 8 shows orientation-dependent, non-spinning ^{13}C spectra, taken at 28°C, of the DPE sample along with one spectrum (*Figure 8A*) of the UDPE sample. Spectra 8A–8D are CP spectra obtained using sequence **I** and spectra 8E–8G show the corresponding NC lineshapes for the DPE sample obtained using sequence **III**. Spectra E–G are arbitrarily normalized to half the intensity of spectra A–D. The average experimental ratios of the intensities of spectra 8E–8G compared with 85–8D are the same as the experimental ratio of the intensities of spectra 5D and 5F, based on the same number of scans. Therefore, it is reasonable to identify the isotropic chemical shift profile of the NC carbons in spectrum 5F with the carbons whose resonances are displayed in spectra 8E–8G. Given that spectrum 5F contains at most a 6% fraction whose resonance profile resembles the crystalline signal, it is fair to say that spectra 8E to 8G show convincing evidence of NC orientation since the NC lineshapes are orientation dependent. Of course, the CP spectra, 8B–8D, show a much stronger orientation dependence because of the more pronounced orientation existing in the crystalline regions.

A measure of the chain axis orientation is the Herman's orientation function[60], F_c defined as

$$F_c = 0.5\ (3 < \cos^2\theta > -1) \qquad (3)$$

where $\langle \cos^2\theta \rangle$ is the ensemble average of individual values of $\cos^2\theta_i$ where θ_i is the angle between the local chain axis direction of the ith chain segment and the macroscopic stretching direction.

The values of F_c can be determined[59] from the first

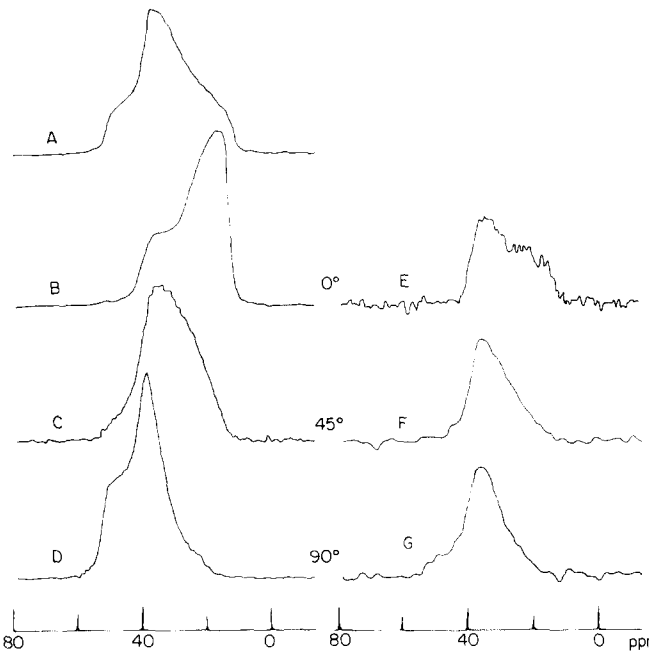

Figure 8 Non-spinning ^{13}C spectra of the UDPE (spectrum A) and the DPE (Spectra B-G) samples. Spectra A–D are CP spectra (Sequence I of *Figure 4*, t_{cp} = 2ms); spectra E–G are NC spectra (Sequence III of *Figure 4*, τ = 10s). The angles given define the angle between the macroscopic draw direction and the static field. The orientation dependence of the total signal (B–D) is certainly stronger than that of the NC lineshapes (E–F). The NC lineshapes have been artificially scaled to 50% of the CP lineshapes. The orientation dependence of the NC lineshapes indicates that the NC chain have preferred orientation

moment, M_1, of the non-spinning ^{13}C lineshape calculated about the mean isotropic chemical shift position. The relationship between M_1 and F_c is

$$M_1 = F_c(\Delta\sigma/3)(3\cos^2\psi - 1) \qquad (4)$$

where $\Delta\sigma$ is the difference between the methylene chemical shift tensor element parallel to the chain axis and the average of the two elements perpendicular to the chain axis; the angle between the macroscopic deformation direction and the applied static magnetic field is ψ. A value of 32.25 ppm was assigned to $\Delta\sigma$[61,62]. The simple form of equation (4) also makes use of the fact that the chain axis coincides with one of the principal axes of the chemical shift tensor in both the OCP of polyethylene[62] and the MCP as evidenced by the C-20 alkane system[61].

Since the NC lineshapes can be isolated (see spectra 8E–8G) and since the isotropic chemical shifts for both the NC lineshape and the CP lineshape can be determined from spectra 5D and 5F, F_c values can be determined independently for both the NC and the combined (OCP plus MCP) crystalline regions; the F_c values are 0.23 ± 0.04 and 0.66 ± 0.06, respectively. If a correction is made to the former value to account for a possible 6% content of crystalline material in the NC lineshape (see *Figure 4F*) whose F_c is that of the crystalline material, then F_c for the NC region becomes 0.20 ± 0.04. The error estimate for the NC F_c value does not take account of ambiguities in the chemical shift anisotropy pattern and the corresponding ambiguities in the definition of the chain axis direction for carbons involved in *gauche* bonds. These complexities are beyond the scope of this paper. There is, however, no error in the choice of σ_{iso} since the centre of gravity of the NC

lineshape can be determined experimentally. That the distribution of chains axis directions in the NC region is not isotropic in this drawn sample remains clear from the orientation dependence of the lineshape.

DISCUSSION

The limit of detectability for the MCP seems to be about 1% using ^{13}C CP-MAS. To a large extent this is due to the downfield tail of the NC signal extending to the downfield side of the OCP line. Quantitative determinations could also be improved slightly by keeping the sample volume considerably smaller than the coil volume in order to avoid signals broadened by insufficient decoupling power[63] arising from those regions near the ends of the RF coil. coil.

The ratio of MCP to OCP will not depend very strongly on achieving an excellent Hartman–Hahn match since, in polyethylene, both the OCP and MCP signals should easily tolerate small mismatches and still cross-polarize fully.

The quantitative character of this CP method using magic-angle sample spinning may not be generally valid. Difficulties could arise in principle if spin-diffusion created a stronger coupling between the crystalline and NC regions. This coupling could be stronger if the NC proton linewidth approaches the crystalline linewidth as is the case in highly drawn polyethylene. Also, if the minimum crystallite dimension between NC surfaces (L_m) becomes small for only one of the crystalline phases, then the assumption of quantitative relative intensities should be reexamined. A possible spectral signature for this condition is that the linewidth of the component having the smaller crystallites would be wider[63]. In any case, if one used a t_{cp} of 0.7 ms the likelihood of getting quantitative relative intensities appears to be excellent except, perhaps, in highly deformed polyethylene where the method might require further scrutiny.

The tentative conclusion was advanced in the n.m.r. results section that if the average L_m values in DPE were greater than 14 nm, then the L_m values were similar for the OCP and the MCP. Examples of (hypothetical) morphologies where L_m is not similar are those cases where one crystalline phase has thinner lamellae or is completely sequestered within the other crystalline phase. Examples of morphologies having similar L_m are (a) separated OCP and MCP crystals having the same or closely similar L_m, or (b) crystals each with a reasonably uniform thickness, containing mixtures of MCP and OCP regions, separated by crystalline defect boundaries along their lateral surfaces.

The basic limitation of the CP method for determining relative MCP and OCP intensities is the magic angle spinning requirement. A detailed study of deformation in UHMWPE would ideally include characterization by X-ray, n.m.r. and electron microscopy techniques. In such a study it would be desirable to examine by n.m.r. polyethylene samples under tension. But maintaining a sample under tension in a high speed rotor is difficult. In principle a small diameter sample could be wound under tension and spun. Another technique called magic-angle hopping[64] has been described but it remains to be seen what spectral resolution can be achieved in this case. The discrete low frequency 'hops' of the latter method, should allow the use of bulkier sample assemblies capable of accommodating specimens under tension.

Finally, we point out that linear polyethylene has been suggested as a useful chemical shift reference for ^{13}C CP-MAS spectra[65]. When samples containing polyethylene are prepared by pressing in a ram press, the MCP is very often visible in the polyethylene reference line. This satellite peak should not be mistaken as indicative of spectrometer malfunction.

CONCLUSIONS

It has been shown that cross-polarization and magic-angle sample spinning ^{13}C n.m.r. techniques can be used to analyse quantitatively the relative amounts of orthorhombic crystalline phase (OCP) and monoclinic crystalline phase (MCP) in UHMWPE. Two samples of UHMWPE were analysed: the first, an undeformed sample UDPE, was slowly cooled from the melt and the second, DPE, was similarly made, and subsequently drawn at room temperature to a strain of 3, and allowed to contract under zero stress to a strain of 1.5. Wide-angle X-ray diffraction indicated that the MCP was absent in the UDPE sample and present in the DPE sample. This was confirmed by the n.m.r. results. The ^{13}C n.m.r. resonance line of the MCP is shifted downfield by 1.4 ppm relative to the OCP resonance in polyethylene. The assignment of the n.m.r. resonance positions was based on similar resonance positions observed in n-alkanes having crystal structures closely related to the two polyethylene crystal phases.

Although the ^{13}C cross-polarization (CP) technique yields distorted relative intensities for the non-crystalline (NC) and crystalline signals, it was shown that the intensities of the OCP and MCP signals were undistorted relative to one another, and that the MCP comprised $8.5 \pm 1\%$ of the crystalline phase in the DPE. The experiments used to demonstrate this also indicated that the spatial distribution of the MCP and the OCP was such that the average distance from MCP protons to their nearest NC-phase protons was approximately the same as from OCP protons to their nearest NC-phase protons. This observation, in turn, is consistent with ideas set forth by other investigators that the MCP is formed by a crystal–crystal transformation in orthorhombic crystalline domains. Evidence pointing to a possible increase in NC-crystal surface area in the DPE sample was also noted.

Orientation was measured using the first moments of the non-spinning ^{13}C n.m.r. lineshapes in the DPE sample. The Hermans orientation function for the combined OCP and MCP regions as well as the NC region was determined. Preferred orientation certainly exists in the NC phase and may be evidence for internal stresses which we presume stabilize the MCP in the DPE.

REFERENCES

1 Pierce Jr., R. H., Tordella, J. P. and Bryant, W. M. D. *J. Am. Chem. Soc.* 1952, **74**, 282
2 Natta, G. *Makromol. Chem.* 1955, **16**, 213
3 Walter, E. R. and Reding, F. P. *J. Polym. Sci.* 1956, **21**, 557
4 Slichter, W. P. *J. Polym. Sci.* 1956, **21**, 141
5 Teare, P. W. and Holmes, D. R. *J. Polym. Sci.* 1957, **24**, 496
6 Frank, F. C., Keller, A. and O'Connor, A. *Phil. Mag.* 1958, **3**, 64
7 Turner-Jones, A. *J. Polym. Sci.* 1962, **62**, 554
8 Seto, T., Hara, T. and Tanaka, K. *Jpn. J. Appl. Phys.* 1968, **7**, 31

9 Hay, I. L. and Keller, A. *J. Polym. Sci.* 1970, **C30**, 289
10 Young, R. J. and Bowden, P. B. *Phil. Mag.* 1974, **29**, 1061
11 Kiho, H., Peterlin, A. and Geil, P. H. *J. Appl. Phys.* 1964, **35**, 1599
12 Bevis, M. and Crellin, E. B. *Polymer* 1971, **12**, 666
13 Allen, P., Crellin, E. B. and Bevis, M. *Phil. Mag.* 1973, **27**, 127
14 Kikuchi, Y. and Krimm, S. *J. Macromol. Sci.-Phys.* 1970, **84**, 461
15 Bowden, P. B. and Young, R. J. *J. Mater. Sci.* 1974, **9**, 2034
16 Bunn, C. W. *Trans. Faraday Soc.* 1939, **35**, 482
17 Nyburg, S. C. and Luth, H. *Acta Cryst.* 1972, **B28**, 2992
18 Crissman, J. M., Passaglia, E., Eby, R. K. and Colson, J. P. *J. Appl. Cryst.* 1970, **3**, 194
19 Nyburg, S. C. and Potworowski, J. A. *Acta Cryst.* 1973, **B29**, 347
20 Broadhurst, M. B. *J. Res. Natl. Bur. Stds.* 1962, **66A**, 241
21 Shearer, H. M. M. and Vand, V. *Acta Cryst.* 1956, **9**, 397
22 Teare, P. W. *Acta Cryst.* 1959, **12**, 294
23 Dawson, I. M. *Proc. Roy. Soc.* (London) 1952, **A214**, 72
24 Khoury, F. A., Fanconi, B. M., Barnes, J. D. and Bolz, L. H. *J. Chem. Phys.* 1973, **59**, 5849
25 Smith, A. E. *J. Chem. Phys. 1953*, **21**, 2229
26 VanderHart, D. L. *J. Magn. Res.* 1981, **44**, 117
27 McKenna, G. B., Khoury, F. A. and Crissman, J. M. *Natl. Bur. of Stds.* Report NBSIR 81-2493 (FDA), 1981
28 Crissman, J. M., Khoury, F. A. and McKenna, G. B. *Natl. Bur. of Stds.* Report NBSIR 82-2493 (FDA), 1982
29 Crissman, J. M., Zapas, L. J. and Khoury, F. A. *Natl. Bur. of Stds.* Report NBSIR 83-2696 (FDA), 1983
30 Trade names of products or equipment are only used for the purpose of identification, this in no way implies endorsement or recommendation by NBS
31 Bacon, D. J. and Geary, N. A. *J. Matls. Sci.* 1983, **18**, 853
32 Alexander, L. E. 'X-ray Diffraction Methods in Polymer Science', Chap. 5, Wiley–Interscience, New York, 1969
33 Gerasimov, V. I. and Tsvankin, D. Ya. *Polym. Sci.* USSR, 1969, **11**, 3013
34 Wilke, W. *Colloid. Polym. Sci.* 1981, **259**, 577
35 Hartmann, S. R. and Hahn, E. L. *Phys. Rev.* 1962, **128**, 2042
36 Pines, A., Gibby, M. G. and Waugh, J. S. *J. Chem. Phys.* 1973, **59**, 569
37 Andrew, E. R. *Arch Sci.* (Geneva) 1959, **12**, 103
38 Schaefer, J., Stejskal, E. O. and Buchdahl, R. *Macromolecules* 1975, **8**, 291
39 Stejskal, E. O., Schaefer, J. and Waugh, J. S. *J. Magn. Res.* 1977, **28**, 105
40 Stejskal, E. O. and Schaefer, J. *J. Magn. Res.* 1975, **18**, 560
41 Earl, W. L. and VanderHart, D. L. *Macromolecules* 1979, **12**, 762
42 Axelson, D. E., Mandelkern, L., Popli, R. and Mathieu, P. *J. Polym. Sci. Polym. Phys. Edn.* 1983, **21**, 2319
43 McCall, D. W. and Douglass, D. C. *Polymer* 1963, **4**, 433
44 Douglass, D. C. and Jones, G. P. *J. Chem. Phys.* 1966, **45**, 956
45 Mansfield, P. and Ware, D. *Phys. Rev.* 1968, **168**, 318
46 Noggle, J. H. and Schirmer, R. E. in 'The Nuclear Overhauser Effect', Academic Press, New York, 1971
47 Alemany, L. B., Grant, D. M., Pugmire, R. J., Alger, T. D. and Zilm, K. W. *J. Am. Chem. Soc.* 1983, **105**, 2133
48 Crank, J. in 'The Mathematics of Diffusion', Clarendon Press, Oxford, 1956
49 Packer, K. J., Pope, J. M., Yeung, R. R. and Cudby, M. E. A. *J. Polym. Sci.*, in press
50 Andrew, E. R. *Prog. Nucl. Magn. Res. Spectrosc.* 1971, **8**, 1
51 Schneider, B., Pivcova, H. and Doskocilova, D. *Macromolecules* 1972, **5**, 120
52 VanderHart, D. L. *Macromolecules* 1979, **12**, 1232
53 Powles, J. G. and Mansfield, P. *Phys. Lett.* 1962, **2**, 58
54 Powles, J. G. and Strange, J. H. *Proc. Phys. Soc.* (London) 1963, **82**, 6
55 Goldman, M. and Shen, L. *Phys. Rev.* 1966, **144**, 321
56 Cheung, T. T. P., Gerstein, B. C., Ryan, L. M., Taylor, R. E. and Dybowski, C. R. *J. Chem. Phys.* 1980, **73**, 6059
57 Hentschel, D., Sillescu, H. and Spiess, H. W. *Macromolecules* 1981, **14**, 1605
58 Assink, R. A. *Macromolecules* 1978, **11**, 1233
59 Hentschel, R., Schlitter, J., Sillescu, H. and Spiess, H. W. *J. Chem. Phys.* 1978, **68**, 56
60 Hermans, J. J., Hermans, P. H., Vermaas, D. and Weidinger, A. *Rec. Trav. Chim.* 1946, **65**, 427
61 VanderHart, D. L. *J. Chem. Phys.* 1976, **64**, 830
62 Opella, S. J. and Waugh, J. S. *J. Chem. Phys.* 1977, **66**, 4919
63 VanderHart, D. L., Earl, W. L. and Garroway, A. N. *J. Magn. Res.* 1981, **44**, 361
64 Bax, A., Szeverenyi, N. M. and Maciel, G. E. *J. Magn. Res.* 1983, **52**, 147
65 Earl, W. L. and VanderHart, D. L. *J. Magn. Res.* 1982, **48**, 35